ORIGINAL PAPER

An Adhesion-Dominated Rolling Friction Regime Unique to Micro-scale Ball Bearings

**Brendan M. Hanrahan · Saswat Misra ·
Mustafa I. Beyaz · Jeremy H. Feldman ·
Christopher M. Waits · Reza Ghodssi**

Abstract We demonstrate that micro-scale rolling bearings exhibit friction and wear properties markedly different from their macro-scale counterparts. A microfabricated testing platform uses variable rolling element diameters or vapor-phase lubricated interfaces to independently test friction force with varying contact area and surface energy. A linear, consistent, relationship between friction force and contact area is observed among different rolling element diameters. When surface free energy is altered through the introduction of vapor-phase lubrication, an 83 % decrease in friction is observed. When coupled with observed ball material adhered to the raceway, there is strong evidence for adhesion-dominated rolling friction regime at the micro-scale.

Keywords Vapor- phase lubrication · Silicon · Ball bearings · Adhesive wear · MEMS

Brendan M. Hanrahan was formerly with Materials Science and Engineering Department, University of Maryland, College Park, College Park, MD, 20704, USA.

B. M. Hanrahan (✉) · C. M. Waits
U.S. Army Research Laboratory, Adelphi, MD 20783, USA
e-mail: brendan.m.hanrahan@gmail.com

Present Address:
B. M. Hanrahan
Oak Ridge Associated Universities Fellowship Program,
Oak Ridge, TN, USA

S. Misra · J. H. Feldman · R. Ghodssi
Electrical and Computer Engineering Department, Institute for Systems Research, University of Maryland, College Park, 2173 A.V. Williams Bldg, College Park, MD 20704, USA
e-mail: ghodssi@umd.edu

M. I. Beyaz
Department of Electrical and Electronics Engineering,
Antalya International University, Antalya, Turkey

1 Introduction

Understanding the friction and wear of new materials and systems is of great importance both scientifically and economically. It is estimated that 6 % of the United States gross domestic product is spent on friction and wear issues including the replacement of worn parts and reduced efficiencies [1]. Bearings, coatings, and lubrication schemes are all employed to help mitigate this issue. Friction and wear properties of interfaces within microsystems have an even greater effect on performance, since surface phenomena gain influence with decreasing size. One approach to addressing friction in these systems, borrowing from the macro-scale, is miniaturized rolling bearings. Experiments show the contributions of surface area and energy to the adhesion mechanisms dictate rolling friction and wear at these size scales. The introduction of vapor-phase lubrication reduced system surface energy and resulted in a six-fold decrease in measured rolling friction. This is the first study on micro-scale rolling contact that links the measured friction to the observed wear mechanisms, providing a comprehensive overview of the adhesive friction properties of micro-scale rolling bearings.

Rolling friction is understood to be the combination of plastic deformation, elastic hysteresis, differential slip, surface adhesion, and other minor components [1–3]. Plastic deformation initially dominates friction for a rolling element in the macro-scale. Once initial deformation of the

surfaces is completed, elastic hysteresis becomes the primary source of rolling friction for steel and ceramic bearing materials [2]. Lubrication is used to reduce corrosion, adhesion, and sliding friction between rolling and auxiliary components (e.g., retainer rings), but has little effect on pure macro-scale rolling friction due to the dominance of elastic hysteresis in these systems. The relative influence of surface and volumetric contributions changes with size scale, as it is well known that miniaturization of linear dimensions results in an accelerated reduction of volumetric property influence when compared to surface properties. Therefore, surface properties will play a disproportionate role in micro-scale systems as compared with the commonly accepted macro-scale rolling friction relationships.

Micro-scale bearings have been employed since the first micro-electromechanical (MEMS) devices had completely released free-moving structures and include sliding, liquid, levitated, and rolling bearings. Sliding bearings were first examined in the MEMS field for use in a variable capacitance micromotor. Although relatively simple to fabricate, these bearings suffered from high friction and wear rates [4]. Liquid bearings use liquid rings or droplets isolated by engineering surface hydrophobicity and are advantageous in that they are inherently low-wear and can dampen vibration from low-stiffness. However, viscosity ultimately limits these bearings to low-speed applications [5, 6]. Levitated bearings prevent solid–solid contact similar to the liquid bearings, using gas or balanced electromagnetic fields to separate moving parts. The levitation method is employed to reduce drag, therefore tailoring levitated contacts to high-speed applications at the expense of stability and complexity [7]. Rolling contact at the microscale has the benefit of high stiffness, low-friction, and low-wear contacts, and is not limited by fabrication complexities inherent to microfabricated non-contact bearings [8].

Microsystems supported on rolling contacts have been demonstrated in a number of power and sensing applications [9–15]. Microball bearings were first used in a linear micro-actuator [11]. Owing to the use of bearings, the linear micro-actuator was modified to become a low frequency vibrational energy harvester with long travel and de-coupled mechanical and electrical properties [13]. To solve problems with stability and integration, an encapsulated version of the microball bearings was created for rotary systems [9]. The encapsulated microball bearings enabled the development of new microturbines, micropumps, micro-motors, and micro-generators. To date, these devices have performed with high speeds and long lifetimes but all suffer from imperfect bearing design and operation with incorrect assumptions regarding the intricacies of micro-scale rolling friction and wear.
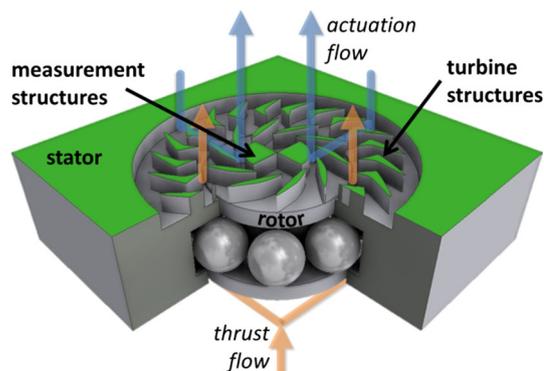

Fig. 1 Schematic of the microturbine device used to test the micro-scale rolling elements. The stator is sectioned to show the ball bearings. Operational flow paths are shown. (Not to scale.)

2 Methodology

A facsimile of the intended application is used as the testing platform to provide the most relevant information. To this end, a microfabricated silicon radial in-flow turbine, shown in Fig. 1, served as the basis for the friction and wear testing to mimic the intended geometries, materials, speeds, and loads for future micro-scale rolling bearing applications. The microturbine platform has been previously used to highlight the relationship between friction torque and normal load [14].

The microturbine testing platform allows for de-coupled speed and normal load control, enabling normal load-resolved friction measurements. The device is fabricated from two single crystalline silicon wafers bonded together to encapsulate the balls in the raceway with deep-etched turbine, alignment, and raceway structures. More information on the device fabrication is presented in Ref. [15] and supplementary material.

The dynamic friction torque (DFT) of the microturbine rotor is a measurement of the spin-down friction torque over the range of rotational frequencies from 1 to 10 krpm. The spin-down testing is performed as follows: first, a normal load is prescribed on the rotor (and thus the rolling elements) through a pressure differential in the device; the rotor then is accelerated to a given rotational frequency through compressed gas passing through etched turbine structures; and finally, actuation flow is discontinued and the rotor decelerates under load. The friction torque is the product of the angular deceleration and the mass moment of inertia, which is calculated from device geometries. A representative data set from spin-down testing is presented in Fig. 2.

The data provided by the spin-down procedure are a combination of micro-scale rolling friction convoluted with all the non-conservative forces within the system including viscous drag in the turbine structure, random interactions between the microballs and sidewalls, gyroscopic spin of
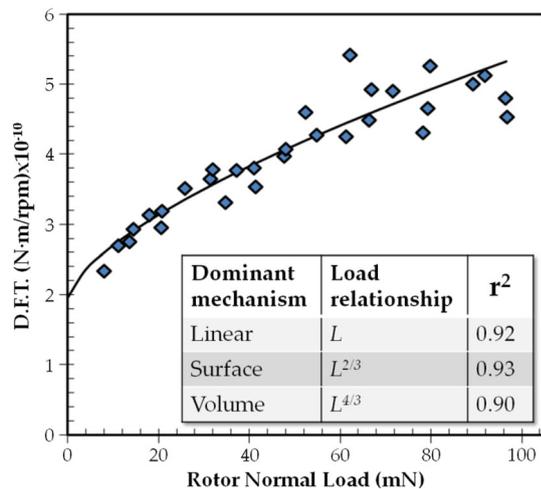
Fig. 2 Dynamic friction torque (DFT) data taken from normal-load resolved spin-down testing of a microturbine supported on microball bearings. (*inset*) Curve-fitting based on surface dominated friction best correlates with the data

the bearing elements, and other contributions. To determine the rolling friction contribution, the relationship between friction torque and normal load was examined. The spin-down procedure was repeated for a range of rotor normal loads from 5 to 100 mN.

In contrast to previously published studies on microball bearing friction, our experiments revealed a new load dependence of friction torque with respect to normal load as well as the likely existence of a load-independent contribution to friction torque, arising from the testing platform, leading to a relationship with DFT of the form:

$$\text{DFT} = \alpha L^{\frac{2}{3}} + \beta \tag{1}$$

where α is a constant depending on materials and geometries, β is the load-independant contributions to friction torque, and L is rotor normal load. The $L^{2/3}$ curve fit relationship including the load independent variable has been displayed in Fig. 2. The $L^{2/3}$ curve fit had the highest coefficient of determination among linear (L), surface ($L^{2/3}$), and volumetric-dominated friction ($L^{4/3}$) functions, and was selected based on the description of the contact area of a sphere on a flat plane in Hertzian contact mechanics [16]. This is analogous to the geometry of the microfabricated raceway-ball bearing system employed in the microturbine, and implies that friction is dominated by contact area-dependant contributions.

The correlation between contact-area and micro-scale rolling friction suggests adhesion is the dominant contribution to friction. Experiments were designed to isolate contact area and adhesion energy variables within the testing platform to test this hypothesis. To isolate contact area, devices were designed to use either 285- or 500-μm

balls, with the raceway altered accordingly, and either 75 %- or 95 %-full packing density of balls in raceways. Ball diameter was chosen based on commercially available options in the <500 μm range, compatible with standard silicon wafer thickness, and a packing density was selected to provide distinct total contact areas while avoiding excess instability from under-packed bearings. The load on the rotating structure was distributed among various sizes and number of rolling elements, allowing for the testing of four different rolling element contact areas among similar platforms. To modify adhesion energy, a system was constructed to deliver controlled saturations of vapor-phase lubrication to the microturbine. During the spin-down deceleration test, normal load is provided by a constant flow into a thrust plenum. This flow passes through the ball bearing raceways and was used to constantly replenish adsorbed lubricant, altering the surface chemistry, and thus, energy of the rolling elements without changing their mechanical properties. By specifically focusing on contact area and adhesion energy, experiments provide multiple mechanisms to discover fundamental friction properties in the tested microsystems.

Adhesive friction can be described by the following: as the element rolls, the leading edge is attracted to the substrate and creates an adhesive joint between the rolling element and substrate. The bond is broken at the trailing edge of the rolling element where the movement of the ball and the attractive forces of the surfaces act in opposition. Friction models have described this process as a continuous crack propagation or an asymmetry in the energy of creation or destruction of the adhesive joint [17, 18]. Using conservation of energy, rolling friction, F_{R}, can be described as the difference of the surface energy of bonded or broken surfaces,

$$F_{\text{R}} = a(\gamma_{12} - \gamma_{1+2}) \tag{2}$$

where a is the radius of contact, γ_{12} is the energy of the bonded surfaces 1 and 2 per unit contact area, and γ_{1+2} is the sum of the energy of the free surfaces per unit contact area. This simplified treatment of adhesive rolling friction contains several components that allow for the analysis of rolling friction, including linear dependence of adhesive friction with contact area, as well as the energy itself, which has been shown to vary with surface chemistry and dwell time [17].

3 Results and Discussion

The correlation between friction and contact area can be calculated from the DFT data of the four microturbine configurations. The prescribed rotor normal load and
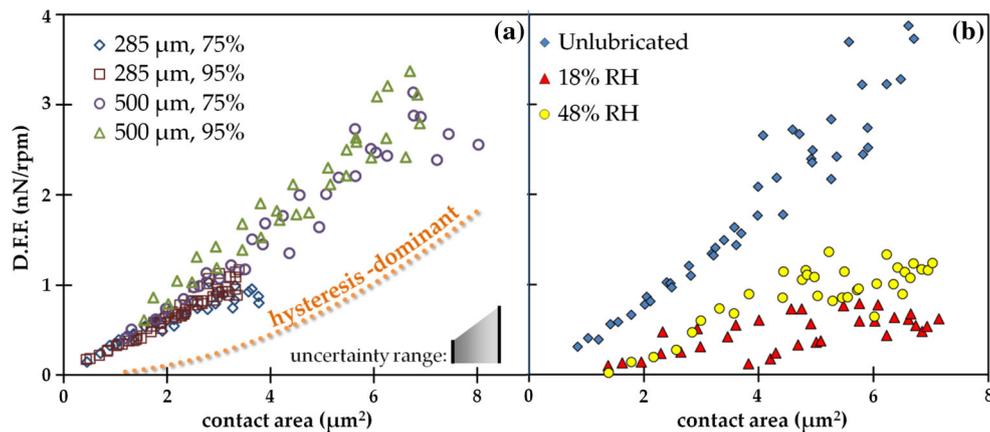
Fig. 3 Dynamic friction force (DFF) relationships with ball contact area for **a** variations of contact area through the use of 285- or 500-μm ball bearings, packed to 75 % or 95 % of a full raceway showing a consistent, linear relationship with contact area and **b** variation of vapor-phase water lubrication concentration, displaying significantly different DFF values. Uncertainty varies with experiment conditions where minimum contact area experiments have minimum uncertainty

known material properties and geometries provide the contact radius, a, using Hertz's equation, assuming no deformation of the contact due to adhesion,

$$a = \left(\frac{3L_B R}{4E^*}\right)^{\frac{1}{3}} \tag{3}$$

where L_B is the load per ball, E^* is the composite elastic modulus, calculated from the modulus and Poisson ratio of the contacting pair, and R is the radius of the ball [16]. Contact area is calculated from the radius assuming circular contact geometry. The DFT is reduced to dynamic friction force (DFF) by first subtracting the load-independent variable, β, obtained from the curve fit of DFT versus normal load data for each device (Eq 1). Then, dividing the load-dependent torque value by the rotor radius results in the total load-dependent dynamic friction force, which is assumed to be uniformly distributed among the balls. DFF is shown to have a linear dependence with contact area in Fig. 3a for all devices, indicating the source of rolling friction is consistent.

Variation in the correlation coefficient among the devices was measured to be 42 % among the 285-μm ball systems and 19 % between the 500-μm ball systems, and 54 % between the two systems. The variation between the systems can be accounted for in the different mass of the balls. The main source of this variation is likely ball-to-sidewall interactions, in which the larger balls carry higher centripetal loads for the same velocity and turn radius compared to the smaller balls. The minor variations in raceway geometry make it challenging to calculate the retarding force that sidewall interacting balls are placing on the system, though the observed trend of increasing mass with friction is consistent with this theory.

The DFF is also shown in Fig. 3b for a microturbine operated under dry, 18 % relative humidity, and 48 % relative humidity conditions. Previous literature has shown that the adhesive energy of a contact can be significantly reduced through the introduction of a lubricant delivered on the surface from the vapor-phase [19–21]. The linear relationship between DFF and contact area is maintained in this study and the fitting coefficient of each condition signifies the varying strength of adhesive energy, both of which support that adhesion is a dominant contribution to friction force. The unlubricated sample has the highest adhesive energy, as expected, with 48 % RH and 18 % RH following in that order, in agreement with published work on relative humidity and adhesive energy [22].

A comparison of Fig. 3a, b reveals features that are unique to the micro-scale rolling friction regime and implicate adhesion as the major contribution. First is the linearity of the friction/contact area relationship in both studies. If micro-scale rolling friction was dominated by volumetric phenomena such as elastic hysteresis, then this relationship would exhibit a *contact area*^{2} relationship owing to the *load*$^{4/3}$ dependence of friction torque for hysteresis systems [2]. This fit relationship is displayed on Fig. 3a for visual comparison. Similarly, if the measured DFT data displayed a linear (Amonton) relationship with normal load then the DFF relationship would scale with *contact area*$^{3/2}$. Figure 3a depicts only the stainless steel and silicon friction couple with no alteration in surface chemistry and shows a similar correlation coefficient among all of the devices with minor deviations described previously. This suggests the underlying source of friction is the same among these devices. This is in contrast to the vapor-lubricated system portrayed in Fig. 3b, which uses surface-assembled molecules to specifically vary the

adhesive energy while maintaining the geometries and mechanical properties of the system. The difference in the correlation coefficient is a factor of 6 between the *Unlubricated* and *18 % RH* lubricated device and 3.3 between *Unlubricated* and *48 % RH*. This method of lubrication would have had negligible effect on a system dominated by elastic hysteresis or plastic deformation. These studies taken together show that adhesion is dominating in the load-dependent component of the measured rolling friction force.

In addition to the adhesion mechanism, there are numerous minor sources of rolling friction in this study arising from the testing apparatus, procedures, and interactions between the ball and raceway. These include viscous drag in the journal bearings and turbine structure, gyroscopic forces acting on the balls, and sliding. The viscous drag component of the friction torque follows Eq 4, Petroff's equation describing a viscous torque in a journal bearing,

$$M_{vis} = \frac{\eta A v r}{d} \qquad (4)$$

where η is the kinetic viscosity of the fluid, in this case nitrogen gas, A is the surface area of concentric cylinders, r is the radius of the rotor and d is the journal bearing gap. These effects have been numerically modeled and contribute about 1 % to the measured friction torque due to the low relative velocities and areas, and larger gaps between parallel areas. Torque due to the gyroscopic effect is calculated from Eq 5 from [23] to be, at most, four orders of magnitude lower than measured torque for a turbine rotating at 10 krpm.

$$M_{gyr} = I \omega_{rotor} \omega_{ball} \qquad (5)$$

where I is the moment of inertia of the ball, ω_{rotor} is the angular velocity of the rotor, and ω_{ball} is the angular velocity of the ball. The influence of sliding or pivoting is difficult to discern. Pivoting will take place on the load-bearing raceways while centripetal force will encourage ball-to-sidewall contact scaling with ω_{rotor}^2. These contributions cannot be directly de-convoluted from the measured friction torque, but it can be inferred their influence in minor due to the measured $L^{2/3}$ friction relationship with contact area, which would be linear otherwise. Also, sliding-dominant friction would not have had a significant reduction of friction with the introduction of vapor-phase lubrication, as observed.

The wear mechanisms observed in the micro-scale rolling bearings are the consequence of adhesion-dominated friction. The primary source of wear was the presence of adhered ball material on the raceway. Figure 4 demonstrates the topography of a wear track obtained by optical interferometric profilometry. The load bearing
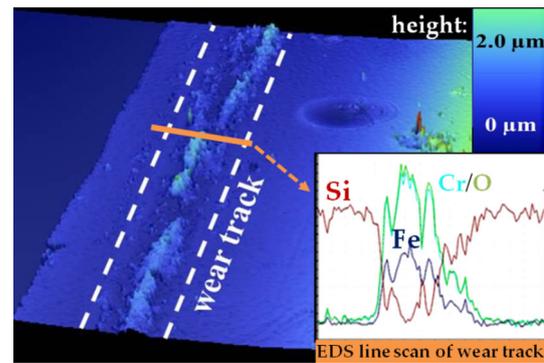

Fig. 4 Topography of wear track obtained through optical profilometry (*inset*) EDS chemical spectrum of scan perpendicular to wear track, exhibiting iron and chromium ball material

surfaces exhibit a near-continuous 20-μm-wide track of additive wear debris. The chemical composition of the wear track was determined using electron dispersive X-ray spectroscopy (EDS). Figure 4 (inset) shows linear-scan spectra taken perpendicular to the wear track with the presence of iron, chrome, and oxygen through the worn area. Inspection of the microballs after testing revealed the source of the adhered wear debris. Pits of removed material were distributed uniformly around the ball with no evidence of adhered silicon raceway silicon on the ball.

The profile in Fig. 4 was obtained in an accelerated wear experiment where the microturbine was operated at a 200-mN rotor normal load over a duration of 20 million revolutions without failure or significant degradation. Beyond the testing shown in the previous figure, further experiments showed that an initial volumetric wear rate of 4×10^{-4} μm^3/mN·rev reduced by an order of magnitude for higher loads and higher revolutions. In the long term, the adhesive wear rate is expected to reach a virtual equilibrium.

At equilibrium, the contact path in the raceway has been coated with ball material. The wear, however, does not arrest; it takes place via a ball material transfer. The ball adheres to ball material on the raceway and fractures in three mechanisms: through the newly formed contact, through the ball (depositing on the raceway), or through the adhered wear track (depositing on the ball). The system is expected to reach equilibrium as the three mechanisms become equally probable, resulting in the net-zero *observed* wear rate for long-term operation once the raceway is coated with ball material.

4 Conclusions

Future systems using micro-scale rolling bearings should be designed to minimize contact area and/or surface free

energy. This is in opposition to macro-scale rolling friction theory where the minimization of contact pressure, and thus maximization of contact area, is desired. The minimum contact area is inherently limited by both the fracture and fatigue characteristics of the coupled materials as well as the roughness of the elements. Surface free energy can be addressed in a number of ways, through the use of lubrication, solid film coatings, or the selection of appropriate material couples. Vapor-phase lubrication is preferred over liquid lubrication due to the lack of capillary forces and capability to perform at high temperatures. Solid film coatings are compatible with microfabrication processes but often times need replenishment, but may find use in applications requiring low lifetimes. Low surface free energy materials, such as ceramics, could offer low friction and wear compared to the stainless steel and silicon materials used in this study.

We have determined the fundamental tribological characteristics of rolling bearings designed to enable future microsystems. The linear relationship between DFF and contact area shows that micro-scale rolling friction arises from a surface-property. Multiple devices using identical materials systems but different geometries show similar adhesion coefficients, suggesting uniform underlying phenomena. When vapor-phase lubrication is introduced, up-to a six-fold reduction in friction force is observed for a system previously operated without lubrication by altering the surface energy but not changing the geometrical properties of the raceway. Finally, the primary wear mechanism of these systems is shown to be the adhesion of ball material on the raceway. Taken together, the contact area, surface energy, and observed wear data show that adhesion is the dominant friction mechanism for the micro-scale rolling bearings. This is the first study to specifically address rolling-friction, wear, and lubrication on the micro-scale, concluding adhesive friction was dominant, thus providing a framework for improving future microsystems through the use of adhesion mitigating schemes.

References

1. Eldredge, K.R., Tabor, D.: The mechanism of rolling friction. I. The plastic range. Proc. Royal Soc. A **229**(1177), 181–198 (1955). doi:10.1098/rspa.1955.0081

2. Tabor, D.: The mechanism of rolling friction. II. The elastic range. Proc. Royal Soc. A **229**(1177), 198–220 (1955). doi:10.1098/rspa.1955.0082

3. Tabor, D.: Elastic work involved in rolling a sphere on another surface. Brit. J. Appl. Phys. **6**, 79–81 (1955)

4. Mehregany, M., Senturia, S.D., Lang, J.H.: Friction and wear in microfabricated harmonic side-drive motors. In: IEEE (ed.) Solid-State Sensor and Actuator Workshop, 1990. 4th Technical Digest., IEEE, Hilton Head, SC, 4-7 Jun 1990 (1990), pp. 17–22. Transducers Research Foundation

5. Yoxall, B.E., Chan, M.L., Harake, R.S., Pan, T.R., Horsley, D.A.: Rotary liquid droplet microbearing. J. Microelectromech. Syst. **21**(3), 721–729 (2012). doi:10.1109/jmems.2012.2185218

6. Chan, M.L., Yoxall, B., Park, H., Kang, Z.Y., Izyumin, I., Chou, J., Megens, M.M., Wu, M.C., Boser, B.E., Horsley, D.A.: Design and characterization of MEMS micromotor supported on low friction liquid bearing. Sens. Actuators A Phys. **177**, 1–9 (2012). doi:10.1016/j.sna.2011.08.003

7. Frechette, L.G., Jacobson, S.A., Breuer, K.S., Ehrich, F.F., Ghodssi, R., Khanna, R., Wong, C.W., Zhang, X., Schmidt, M.A., Epstein, A.H.: High-speed microfabricated silicon turbomachinery and fluid film bearings. J. Microelectromech. Syst. **14**(1), 141–152 (2005). doi:10.1109/jmemes.2004.839008

8. Ghodssi, R., Hanrahan, B., Beyaz, M.: Microball bearing technology for MEMS devices and integrated microsystems. In: IEEE (ed.) 16th International Conference on Solid-State Sensors, Actuators, and Microsystems (Transducers 2011), Beijing, China, June 5-9, (2011), pp. 1789–1794

9. Waits, C.M., McCarthy, M., Ghodssi, R.: A microfabricated spiral-groove turbopump supported on microball bearings. J. Microelectromech. Syst. **19**(1), 99–109 (2010)

10. Waits, C.M.: A low-wear planar-contact silicon raceway for microball bearing applications. In: U.S. Army Research Laboratory Technical Report, ARL-TR-4796. vol. ARL-TR-4796 (2009)

11. Ghalichechian, N., Modafe, A., Lang, J.H., Ghodssi, R.: Dynamic characterization of a linear electrostatic micromotor supported on microball bearings. Sens. Actuators A Phys. **136**(2), 496–503 (2007)

12. Ghalichechian, N., Modafe, A., Beyaz, M.I., Ghodssi, R.: Design, fabrication, and characterization of a rotary micromotor supported on microball bearings. J. Microelectromech. Syst. **17**(3), 632–642 (2008)

13. Naruse, Y., Matsubara, N., Mabuchi, K., Izumi, M., Suzuki, S.: Electrostatic micro power generation from low-frequency vibration such as human motion. J. Micromech. Microeng. **19**(9), 094002 (2009)

14. McCarthy, M., Waits, C.M., Ghodssi, R.: Dynamic friction and wear in a planar-contact encapsulated microball bearing using an integrated microturbine. J. Microelectromech. Syst. **18**(2), 263–273 (2009)

15. McCarthy, M., Waits, C.M., Beyaz, M.I., Ghodssi, R.: A rotary microactuator supported on encapsulated microball bearings using an electro-pneumatic thrust balance. J. Micromech. Microeng. **19**(9), 094007 (2009)

16. Hertz, H.: On the contact of rigid elastic solids. Gesammelte Weke **1**, 155–195 (1895)

17. Kendall, K.: Rolling friction and adhesion between smooth solids. Wear **33**(2), 351–358 (1975)

18. Johnson, K.L.: Mechanics of adhesion. Tribol. Int. **31**, 413–418 (1999)

19. Asay, D.B., Kim, S.H.: Effects of adsorbed water layer structure on adhesion force of silicon oxide nanoasperity contact in humid ambient. J. Chem. Phys. **124**(17), 174712 (2006). doi:10.1063/1.2192510

20. Asay, D.B., Dugger, M.T., Ohlhausen, J.A., Kim, S.H.: Macro- to nanoscale wear prevention via molecular adsorption. Langmuir **24**(1), 155–159 (2007). doi:10.1021/la702598g

21. Asay, D., Dugger, M., Kim, S.: In-situ vapor-phase lubrication of MEMS. Tribol. Lett. **29**(1), 67–74 (2008). doi:10.1007/s11249-007-9283-0

22. Jones, R., Pollock, H.M., Cleaver, J., Hodges, C.: Adhesion forces between glass and silicon surfaces in air studied by AFM: Effects of relative humidity, particle size, roughness, and surface treatment. Langmuir **18**, 8045–8055 (2002)

23. T. A. Stolarski, S.T.: Rolling contacts. Tribology in practice series. Professional engineering publications, (2001)